



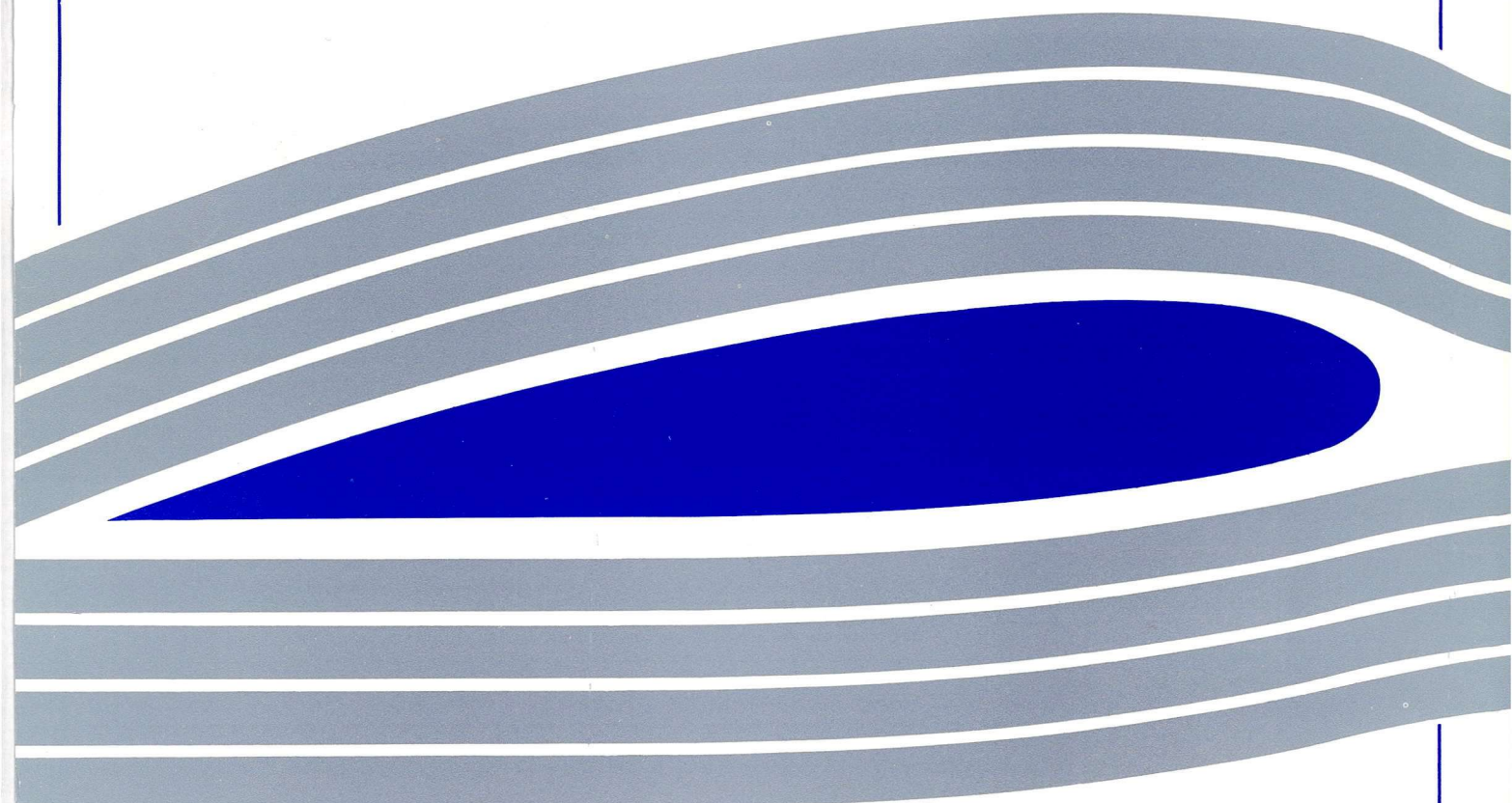
University of Glasgow  
DEPARTMENT OF  
**AEROSPACE  
ENGINEERING**



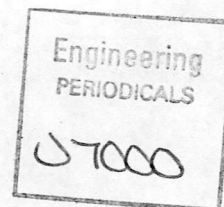
Engineering  
PERIODICALS

57000

The Simulation of Recovery Procedures  
from Engine Failures During Helicopter  
Offshore Operations







The Simulation of Recovery Procedures  
from Engine Failures During Helicopter  
Offshore Operations

by

C. D. Taylor, D. G. Thomson and R. Bradley

Internal Report No. ~~2310~~ 9331

Department of Aerospace Engineering  
University of Glasgow  
Glasgow G12 8QQ

September 1993







## Summary

This report discusses the mathematical models and the specialised simulation techniques developed for an investigation of helicopter offshore operations under adverse conditions. The development of a mathematical model of a torque limited, twin engine power plant capable of accommodating multiple or single gas turbine failures is presented. In order to simulate engine failures during the critical phases of takeoff or landing manoeuvres, a novel hybrid simulation technique called HIFIS which incorporates both inverse and forward methods has been developed. Its formulation and the subsequent specialised recovery trajectories that it requires are detailed.



## **Contents**

### **1.0 Introduction**

### **2.0 Twin Engine Model**

#### **2.1 Mathematical Formulation of Multiple Engine Power Plant**

### **3.0 Simulation of Recovery from Engine Failure**

#### **3.1 Discussion of HIFIS Algorithm**

#### **3.2 Definition of Recovery Manoeuvres**

##### **3.2.1 Recovery Manoeuvre Requirements**

##### **3.2.2 Mathematical Formulation of Recovery Manoeuvres**

### **4.0 Conclusions**

### **Acknowledgements**

### **References**

### **Figures**





## Nomenclature

$K_{e1}$	Gains associated with change in rotor speed	(kg/rad)
$K_{e2}$	Gains associated with change in engine torque	(Nms/kg)
$K_3$	Overall gain of engine governing system	(Nms/rad)
$Q_E$	Engine torque	(Nm)
$Q_{E \text{ IDLE}}$	Engine torque at flight idle	(Nm)
$Q_{E \text{ LIM}}$	Maximum single engine torque output	(Nm)
$Q_{E \text{ MAX}}$	Total maximum allowable engine torque	(Nm)
$Q_R$	Main rotor torque	(Nm)
$Q_{TR}$	Tail rotor torque	(Nm)
$s$	Laplace operator	
$t$	Time	(s)
$t_{\text{fail}}$	Engine failure time	(s)
$t_m$	Manoeuvre time	(s)
$t_{\text{pr}}$	Pilot response time	(s)
$t_R$	Recovery manoeuvre time	(s)
$t_r$	Pilot reaction time to engine failure	(s)
$w_f$	Fuel flow	(kg/s)
$w_{f \text{ IDLE}}$	Fuel flow at flight idle	(kg/s)
$x, y, z$	Component of flight path co-ordinates	(m)

## Greek Symbols

$\delta_x, \delta_y, \delta_z, \delta_\psi$	Recovery lag	
$\Omega$	Angular velocity of rotor	(rad/s)
$\Omega_{\text{IDLE}}$	Angular velocity of rotor at flight idle	(rad/s)
$\Omega_{Q_{\text{MAX}}}$	Angular velocity of rotor at maximum engine torque	(rad/s)
$\dot{\Omega}$	Angular acceleration of the rotor	(rad/s <sup>2</sup> )
$\tau_{e1}, \tau_{e2}, \tau_{e3}$	Time constants associated with engine governor	(s)





## 1.0 Introduction

The work documented in this report is part of a study at the University of Glasgow investigating helicopter offshore operations. Research in the past has been aimed at the enhancement of rotor inflow modelling and the mathematical representation of helicopter offshore manoeuvres and these studies are the topics of two previous publications Refs.[1] and [2]. Current investigations have concentrated on helicopter performance and pilot strategy when a single engine failure occurred during the key phases of either takeoff or landing manoeuvres. Originally, the study of offshore operations that included the aircraft suffering an engine failure was undertaken using Helinv, Ref.[3], a software package capable of performing inverse simulation. Inverse simulation is ideally suited to offshore operations as the manoeuvre trajectory effectively becomes the input to the simulation allowing the vehicle states and control displacements to be evaluated. It was evident from the early stages of the study that the existing Helinv algorithm would require modification if the aims of the investigation were to be met. This report details the new limitations and the methods used to meet them.

The mathematical model of the helicopter utilised in the Helinv algorithm has provision for single engine operation only - without either a power limiting structure or capability to simulate multiple or individual engine failures. From the inception of the current study, the importance of the ability to simulate engine failures and to limit the available engine torque output was fully appreciated. For the original version of Helinv during the period of flight where an engine failure was experienced, the unlimited engine torque output of the remaining engine would lead to the generation of unrealistic piloting strategies and performance capabilities of the vehicle. The development of a more realistic mathematical model of a twin engine, torque limited powerplant capable of accommodating multiple or single gas turbine failures is detailed in section 2 of this document.

The need to take into account the pilot's reaction time in the event of an engine failure has also been addressed. As an example, consider the case of a takeoff manoeuvre, where an engine failure at some critical point is to be simulated. With inverse simulation, the whole manoeuvre is predefined, so that after the engine failure point, the simulation continues with modified engine characteristics. This formulation does not represent the actual situation as it assumes an ideal pilot who can react instantaneously to the new situation. A better approach is to allow the pilot to continue with his original strategy assuming no engine failure but applying it to a helicopter with changing dynamic characteristics (due to the engine failure) until the reaction time has elapsed. During the





reaction interval, the helicopter may depart from the commanded trajectory so that a new piloting strategy is required to return the helicopter to its original trajectory, or to some new recovery flight path. The capturing of this new strategy into the derivation of the new flight path is one of the main modelling problems requiring attention. Through careful application of conventional and inverse simulation methods, a novel hybrid simulation technique that incorporates both inverse and forward methods has been developed, enabling variations in pilot response time to be accommodated. The formulation of this algorithm and the subsequent specialised 'recovery' trajectories required are detailed in section 3.

## **2.0 Twin Engine Power Plant**

Helicopters conducting offshore operations over waters governed by the United Kingdom must comply with the Category A safety regulations outlined by the Civil Aviation Authority and documented in Ref.[4]. The Category A specifications dictate that the vehicle must be of multi-engine design with independent engines, fuel and electrical systems. The engine's power limits specified by the manufacturer must be adhered to under normal operating conditions, preventing both gearbox overload or failure and reduced engine fatigue life. Furthermore, any single failure of either the engine or its ancillary systems can not cause a failure of another engine. The remaining engine must satisfy an emergency power structure such as that outlined in Ref.[5], where additional power is available for small periods of time to allow continued and safe flight of the helicopter.

Helinv utilises the helicopter mathematical model HGS, Ref. [6]. Given the CAA limitations outlined above, it would be desirable for HGS to have the provision of multiple engine operation, limited torque output and in addition, the facility to simulate an engine failure. In its original form, none of these characteristics were available within HGS and it was evident that both a more flexible and sophisticated engine representation would be required.

The mathematical modelling of multiple gas turbine type power plants can be achieved by several means. A simple method is to assume that the independent engines can be combined as a single power source, controlled by two independent hydromechanical governing mechanisms. This method is very useful as it requires little engine characteristic data and fits readily into current simulation packages, however it greatly underestimates the physical and thermodynamic concepts of an operating gas turbine. More sophisticated engine models are available - for example,





'The Inter Component Volume (ICV) Method' detailed in Ref.[7]. Such models can be computationally intensive, and require knowledge of many physical parameters. Consequently they were judged unsuitable for the current investigation.

The approach of representing the gas turbine engines as a single power source was selected for this study on the grounds that its efficiency and economy was better suited to the flight mechanics (rather than thermodynamic) study being undertaken. The model adopted is a development of the single engine model presented by Padfield, Ref.[8]. The mathematical formulation of the twin engine, torque limited power plant is detailed in the following section.

## 2.1 Mathematical Formulation of Twin Engine Power Plant

Prior to detailing the twin engine, torque limited model it is useful to recall Padfield's single engine model.

In the single engine power plant, the engine torque,  $Q_E$ , is related to the rotor speed,  $\Omega$ , by the following,

$$\dot{\Omega} = (Q_E - Q_R - G_{TR} Q_{TR}) / I_{TR} + \dot{i} \quad (1)$$

where  $Q_R$  and  $Q_{TR}$  are the main and tail rotor torque's respectively,  $G_{TR}$  the tail rotor gear ratio,  $I_{TR}$  is the sum of the main rotor, tail rotor, and transmission polar moments of inertia, and  $\dot{i}$ , the yaw component of angular acceleration.

The engine torque is automatically controlled by a governing system that relates changes in rotor speed,  $\Delta\Omega$ , to changes in fuel flow,  $\Delta w_f$ . This part of the governing system is specified in terms of a simple first order lag with gain  $K_{e1}$  and time constant  $\tau_{e1}$ . Its transfer function has the form,

$$\frac{\Delta w_f}{\Delta\Omega} = \frac{K_{e1}}{1 + \tau_{e1} s} \quad (2)$$

The increment in fuel flow change and rotor speed are given by,

$$\Delta w_f = w_f - w_{f \text{ IDLE}}$$

and,





$$\Delta\Omega = \Omega - \Omega_{IDLE}$$

where  $w_{fIDLE}$  and  $\Omega_{IDLE}$  are the fuel flow and main rotor speed at flight idle. The second part of the governing system relates the changes in fuel flow to changes in engine torque,  $\Delta Q_E$  and has the form,

$$\frac{\Delta Q_E}{\Delta w_f} = K_{e2} \left( \frac{1 + \tau_{e2} s}{1 + \tau_{e3} s} \right) \quad (3)$$

where,

$K_{e2}$  is the gain associated with the engine response to fuel flow,

$\Delta Q_E$  the change in rotor torque from flight idle ( $\Delta Q_E = Q_E - Q_{EIDLE}$ ),

$Q_{EIDLE}$  is the rotor torque at flight idle and assumed to have the value  $Q_{EIDLE}=0$ ,

$\tau_{e2}$  and  $\tau_{e3}$  are time constants which are functions of engine torque and are given by,

$$\tau_{e2} = \tau_{e20} + \tau_{e21} \left( \frac{Q_E}{Q_{E MAX}} \right)$$

$$\tau_{e3} = \tau_{e30} + \tau_{e31} \left( \frac{Q_E}{Q_{E MAX}} \right)$$

where  $Q_{E MAX}$  is the maximum allowable engine torque output.

Combining equations (2) and (3) gives the equations of motion of a power plant and for a single engine system can be shown to be of the form (with some manipulation),

$$\ddot{Q}_E = \frac{1}{(\tau_{e1} \tau_{e3})} \left( -(\tau_{e1} + \tau_{e3}) \dot{Q}_E - Q_E + K_3 (\Omega - \Omega_{IDLE} + \tau_{e2} \dot{\Omega}) \right) \quad (4)$$

where,

$$K_3 = K_{e1} K_{e2}$$



Equations (1) and (4) represent a single engine free turbine power plant. This model has no provision for limiting the torque available from the engine and consequently whatever torque is demanded by the rotors is supplied by the engine via the governor. An example of the response of this model to a step input in engine torque demand is shown in Figure 1. The integration of equations (1) and (4) was achieved by use of a fourth order Runge-Kutta scheme. Initially the torque demand is 5kNm, and after one second, torque required from the engine is increased to 10kNm. It should be noted that the maximum available torque output,  $Q_{E_{MAX}}$  in this case was specified to be 7.5kNm.

To modify the existing engine model for the twin engine case, the first step is to rewrite equation (1) as,

$$\dot{\Omega} = (Q_{E_1} + Q_{E_2} - Q_R - G_{TR} Q_{TR}) / I_{TR} + \dot{r} \quad (5)$$

where  $Q_{E_1}$  and  $Q_{E_2}$  denote the contributions of engine torque output from both engine one and two respectively. The function of varying fuel flow in response to changes in rotor speed in the engine governor is modelled by equation (2). A reasonable assumption is that each engine of a twin gas turbine powerplant will consume fuel at half the rate of an equivalent single engine plant and therefore,

$$K_{el(i)} = \frac{1}{2} K_{el} \quad i=1,2$$

Furthermore, the fuel flow module will supply fuel at a sufficient rate to allow any torque demanded to be supplied by the engines and this is demonstrated by Figure 1. In a real gas turbine engine, there is only a finite power output available (usually specified by the manufacturer, although in helicopters maximum available torque is usually limited by the main rotor gearbox). The limiting of the torque produced by each engine is achieved by setting a limit on the fuel flow rate that the engine governing system can deliver. First, write equation (2) as,

$$\frac{\Delta w_f^*(i)}{\Delta \Omega^*} = \frac{1}{1 + \tau_{el} s} \quad (6a)$$

or alternatively,





$$\Delta \dot{w}_f^* (i) = \frac{-(\Delta w_f^* (i) - \Delta \Omega^*)}{\tau_{e1}} \quad (6b)$$

where,

$$\Delta w_f^* (i) = \frac{\Delta w_{f(i)}}{K_{e1(i)}} \quad (6c)$$

and  $\Delta \Omega^*$  represents the difference in rotor speed is defined according to the fuel flow schedule. The construction and implementation of the fuel schedule is discussed later in this section.

Now rewrite equation (2) for the multiple engine case and substitute equation (6c) to give,

$$\frac{\Delta Q_{E(i)}}{\Delta w_f^* (i)} = K_{3(i)} \left( \frac{1 + \tau_{e2(i)} s}{1 + \tau_{e3(i)} s} \right) \quad (7)$$

where the time constants  $\tau_{e2(i)}$  and  $\tau_{e3(i)}$  are given by,

$$\tau_{e2(i)} = \tau_{e20} + \tau_{e21} \left( \frac{Q_{E(i)}}{Q_{E \text{ LIM}}} \right)$$

$$\tau_{e3(i)} = \tau_{e30} + \tau_{e31} \left( \frac{Q_{E(i)}}{Q_{E \text{ LIM}}} \right)$$

and,

$$K_{3(i)} = K_{e1(i)} K_{e2}$$

$$Q_{E \text{ LIM}} = \frac{1}{2} Q_{E \text{ MAX}}$$

Manipulation of equation (7) and remembering  $Q_{E \text{ IDLE}} = 0$ , yields,

$$\dot{Q}_{E(i)} = \frac{1}{\tau_{e3(i)}} \left( K_{3(i)} (\Delta w_f^* (i) + \tau_{e2(i)} \Delta \dot{w}_f^* (i)) - Q_{E(i)} \right) \quad (8)$$





With respect to the fuel schedule, it is assumed to be a function of the difference in actual and flight idle rotor speed,  $\Delta\Omega$ . At the condition of maximum torque output from the gas turbine, the fuel flow to the engine will be at a maximum constant level. Furthermore the rotor speed will have dropped below a certain minimum level denoted by,  $\Omega_{Q_{MAX}}$ , giving  $\Delta\Omega^* = \Delta\Omega_{MIN}$  where,

$$\Delta\Omega_{MIN} = \Omega_{Q_{MAX}} - \Omega_{IDLE} \quad (9)$$

so that  $\Delta\Omega_{MIN}$  is naturally a negative quantity. During normal engine torque output operating limits, the fuel schedule is given by,

$$\Delta\Omega^* = \Delta\Omega$$

When rotor speed is greater than the maximum rotor speed, the fuel flow is shut off (so that its value cannot be negative) by setting  $\Delta\Omega^*$  to zero. Hence the three operating conditions of the fuel schedule can be written as,

$$\Delta\Omega^* = \begin{cases} \Delta\Omega_{MIN} & \Delta\Omega_{MIN} \geq \Delta\Omega \\ \Delta\Omega & 0 > \Delta\Omega > \Delta\Omega_{MIN} \\ 0 & \Delta\Omega \geq 0 \end{cases}$$

The variation of fuel flow,  $\Delta w_{f(i)}$ , with rotor speed,  $\Delta\Omega^*$ , is shown graphically in Figure 2.

In constructing the fuel schedule, it is necessary to evaluate the minimum rotor speed at which maximum engine torque output is achieved,  $\Omega_{Q_{MAX}}$ .

Let,

$$\Omega_{Q_{MAX}} = \Omega_{IDLE} \gamma \quad (10)$$

where  $\gamma$  denotes a rotor droop factor. Substituting equation (10) into (9) and rearranging for  $\gamma$  gives,

$$\gamma = \frac{\Delta\Omega_{MIN}}{\Omega_{IDLE}} + 1 \quad (11)$$



Under steady conditions equation (4) reduces to,

$$Q_E = K_3 \Delta\Omega \quad (12)$$

If the power plant is at maximum steady output, then equation (12) can be written as,

$$Q_{E\text{ MAX}} = K_3 \Delta\Omega_{\text{MIN}}$$

and substituting this expression into equation (11) enables the rotor droop factor to be evaluated from,

$$\gamma = \frac{Q_{E\text{ MAX}}}{K_3 \Omega_{\text{IDLE}}} + 1$$

Therefore equations (5), (6b) and (8) represent a twin gas turbine powerplant with a limited power output. An example of the use of this model is shown in Figure 3. In this test case, both engines are initially generating 5kNm torque to met a demand of 10kNm. The maximum available torque from each gas turbine is specified to be 7.5kNm. At  $t=0.5s$ , number two engine is failed and subsequently engine number one begins to increase its torque output to compensate for the reduced net torque output. With the torque required from the powerplant held at 10kNm, it can be seen that the engine governor never permits this torque demand to be met by the remaining engine.

### 3.0 Simulation of Recovery from Engine Failure

The aim of current work is to apply inverse simulation to the study of control strategies in the event of an engine failure. The conventional approach to inverse simulation has been to define a complete manoeuvre, then calculate the required controls to fly it. There are two problems associated with this approach when applied to manoeuvres where engine failures occur:

- i) After engine failure, the performance of the helicopter will be impaired by power and torque limitations and there is no guarantee that the manoeuvre as defined initially can be still be flown.
- ii) Even if the manoeuvre can still be performed, it is unrealistic simply to continue with inverse simulation exactly from failure point, albeit taking into account the effect of





the failed engine. This would assume that the pilot was immediately aware of the engine failure, and was able to compensate for the lost engine infinitely quickly. In effect the time delay due to the pilot's reaction to warning signals etc., has not been included.

To overcome the above problems, a hybrid simulation involving both inverse and conventional time response techniques has been developed along with an algorithm for defining recovery manoeuvres for the situation where the initially defined manoeuvre cannot be completed. The resulting simulation 'HIFIS' (Helicopter Inverse Forward Inverse Simulation) is discussed in the following sections.

### 3.1 Discussion of the HIFIS Algorithm

In essence the problem to be solved is that, it is no longer possible to completely define the whole manoeuvre without consideration of the changes in vehicle dynamics induced by engine failure. The most convenient approach to then take is to consider the manoeuvre as consisting of various phases, and then apply either the forward or inverse simulation as appropriate. The final scheme adopted is as follows:

- i) The complete manoeuvre (a Towering Takeoff for example) is defined over a time interval  $t=0$  to  $t=t_m$  in the usual form, Ref. 2.
- ii) A conventional inverse simulation is used up to the point  $t = t_{pr} = t_{fail} + t_r$ . The implication here is that the engine fails at some time point  $t=t_{fail}$  in the manoeuvre, and it takes the pilot a time  $t_r$  to react to this failure. The justification for the continuation of inverse simulation over the interval  $t=t_{fail}$  to  $t=t_{fail} + t_r$  merits brief discussion. The assumption here is that during this phase the pilot will not have perceived the engine failure and will therefore continue to fly the manoeuvre as if he had full engine power available. The inverse simulation over this phase therefore calculates the control strategy associated with the full twin engine model.
- iii) Before a recovery path can be defined it is necessary to obtain the states and position of the helicopter at the pilot's reaction point. For this information, a conventional time response calculation is employed from  $t=t_{fail}$  to  $t=t_{pr}$  using the control inputs calculated for the non-engine-failure inverse simulation of this phase, but applied to the helicopter mathematical model with the effect of the engine failure included.
- iv) Using the current vehicle earth axis position, velocity and accelerations, the recovery manoeuvre is evaluated from  $t=t_{pr}$  to  $t=t_R$ , where  $t_R$  denotes the recovery





manoeuvre time. Having obtained a mathematical description of the trajectory in a manner described in the following section, it is possible to return to a conventional inverse simulation and obtain the corresponding control strategy.

### 3.2 Definition of Recovery Manoeuvres

#### 3.2.1 Recovery Manoeuvre Requirements

The final phase of the HIFIS program is the inverse simulation of the recovery manoeuvre after the engine failure. It is therefore necessary to formulate mathematical descriptions of these manoeuvres. Emergency procedures and strategies presented in Ref.[4] indicate that the recovery manoeuvre employed should either rejoin the aircraft to its original flight path or be a completely new recovery trajectory. Furthermore the recovery action initiated by the pilot must reflect the helicopters current state of safety both in terms of the position which it holds in the pilot's immediate priorities and the rate with which this action is carried out once initiated. For example, a helicopter experiencing a single engine failure just after the critical decision point would result in the pilot immediately initiating a recovery manoeuvre with rapid execution of a pitch down and descent as is shown in Figure 4. In contrast, a helicopter suffering an engine failure near the end of a Towering Takeoff manoeuvre would possibly result in the pilot initiating recovery action after checking the immediate cause of the failure - with the recovery manoeuvre undertaken as to cause least disturbance to crew and cargo.

To create a mathematical description of a recovery manoeuvre, the problem is one of finding a suitable geometric profile to match defined entry and exit conditions. The entry conditions are defined by the final point on the time response calculation over the period from pilot reaction and response time and in effect represents the deviation from the desired trajectory. The exit conditions are defined (by the user) in terms of a desired altitude, flight velocity, climb rate or some combination of these. It is also desirable that the mathematical representation of the flight paths must encapsulate the initial boundary conditions up to and including at least the jerk components, while preventing the generation of unrepresentative points of inflexion. Furthermore it would be useful if a range of recovery flight paths could be generated that satisfy a single recovery manoeuvre boundary condition set, allowing the influence of pilot strategy to be investigated.

The mathematical formulation of a recovery manoeuvre capable of meeting the requirements outlined above are detailed in the following section.





### 3.4.2 Mathematical Formulation of a Recovery Manoeuvre

The requirement for a recovery manoeuvre is for some function  $h(t)$  that blends smoothly from the trajectory  $f(t)$  resulting from the departure from the desired flight path to some final safe trajectory or condition, (or the original flight path)  $g(t)$ , see Figure 5. The recovery is initiated at the point where the pilot has reacted to the engine failure, and decided upon his strategy for recovery,  $t_{pr}$ . It is assumed that the required final point of the recovery manoeuvre is where the original trajectory (or new trajectory) is reached and this occurs at a time  $t_R$ .

The recovery manoeuvre is completed at time  $t_{pr}$ , at which point either the original trajectory has been regained or a revised trajectory has been joined.

From Figure 5, it is clear that,

$$h(t)=g(t)+\phi(t) \quad (12)$$

where  $\phi(t)$  is the function used to undertake the blending process. The entry ( $t=t_{pr}$ ) and exit ( $t=t_R$ ) conditions to the recovery manoeuvre can be written as,

$$h^m(t_{pr}) = g^m(t_{pr}) + \phi^m(t_{pr}) \quad \text{for } m=0 \text{ to } M$$

and,

$$h^n(t_R) = g^n(t_R) + \phi^n(t_R) \quad \text{for } n=0 \text{ to } N$$

where  $M$  and  $N$  are the degrees of required derivative continuity at  $t=t_{pr}$  and  $t=t_R$  respectively. The blending function also satisfies,

$$\phi^m(t_{pr}) = f^m(t_{pr}) - g^m(t_{pr}) \quad \text{for } m=0 \text{ to } M \quad (13a)$$

and,

$$\phi^n(t_R) = 0 \quad \text{for } n=0 \text{ to } N \quad (13b)$$

A suitable function  $\phi(t)$  for the blend must now be chosen. In previous inverse simulation work, much use has been made of simple polynomials for flight path definition. The





further step of biasing a general polynomial has been taken to allow the variation of speed at which the recovery is undertaken. The general form of the blending function is then,

$$\phi(t) = e^{-\delta t} p(t) \quad (14)$$

where  $p(t)$  is a polynomial whose order is chosen to ensure the required derivative continuity at entry and exit is met (the order is then  $M+N-1$ ), whilst the value  $\delta$  may be varied to influence the rate at which blending is effectively achieved.

Consider the case where continuity up to the third derivative is required at both the entry and exit of the recovery manoeuvre. This gives the boundary conditions:

$$\text{i) } t=t_{pr} \quad p(t)=p(t_{pr}) \quad p'(t)=p'(t_{pr}) \quad p''(t)=p''(t_{pr}) \quad p'''(t)=p'''(t_{pr})$$

$$\text{ii) } t=t_r \quad p(t)=p(t_r) \quad p'(t)=p'(t_r) \quad p''(t)=p''(t_r) \quad p'''(t)=p'''(t_r)$$

and hence the polynomial will take the form:

$$p(t) = a_0 + a_1 t + a_2 t^2 + a_3 t^3 + a_4 t^4 + a_5 t^5 + a_6 t^6 + a_7 t^7$$

Clearly once the values of  $p(t_r)$ ,  $p'(t_r)$ , ...,  $p'''(t_r)$  are known it is a simple case of solving eight simultaneous linear algebraic equations to find  $a_0$ , ...,  $a_7$ . To obtain the values of these boundary conditions, equation (14) must be successively differentiated to give,

$$p(t) = \phi(t) e^{\delta t}$$

$$p'(t) = \phi'(t) e^{\delta t} + \delta \phi(t) e^{\delta t}$$

$$p''(t) = \phi''(t) e^{\delta t} + 2\delta\phi'(t) e^{\delta t} + \delta^2\phi(t) e^{\delta t}$$

$$p'''(t) = \phi'''(t) e^{\delta t} + 3\delta\phi''(t) e^{\delta t} + 3\delta^2\phi'(t) e^{\delta t} + \delta^3\phi(t) e^{\delta t}$$

This results in the required boundary conditions in terms of  $\phi(t)$  and its derivatives, which, at the times  $t=t_{pr}$  and  $t=t_r$ , are given by equations (13a) and (13b). In equation (13a) the values of  $f^m(t_{pr})$  are simply the final conditions of the time response calculation performed over the pilot's reaction time.





For the conditions at the final point there are two options. Firstly, if the blend is to return the helicopter back to the original defined trajectory, then it is simply a case of evaluating  $g(t_R)$ ,  $g'(t_R)$ , etc. from the known profile, see Figure 5. The more likely case is that an alternative flight trajectory will be required simply due to the fact that the original may be unflyable due to the now limited power available. In these circumstances, the new values for  $g(t_R)$  and its derivatives need to be determined. Alternatively, simple acquisition of some predefined flight condition may suffice. For example, recovery from an engine failure after the TDP of a towered takeoff may be considered as the achievement of a steady climb rate at constant heading at some altitude above the sea. Again the values  $g(t_R)$ ,  $g'(t_R)$  etc. are readily found.

An example of a recovery manoeuvre for rejoining a prescribed flight path is now discussed. Figure 6 presents the flight path for a Towered Takeoff manoeuvre. The inverse - forward simulation transition occurs at  $t=20s$  with the forward phase being employed for a duration of 5 seconds (a unrealistically long reaction time has been selected as a demonstration). As mentioned previously, the helicopter will 'drift' a small amount from the desired flight path during the forward phase and this is evident from the plot. For the case when it is necessary to rejoin the original trajectory, an additional blending flight path that provides a smooth transition from the current to the original flight path is required. The longitudinal, lateral and altitude time histories necessary for such a transition are evaluated from equation (14) and shown in Figure 7. The four different data sets correspond to the original trajectory and the three values of the recovery lags,  $\delta_x$ ,  $\delta_y$  and  $\delta_z$ . The benefit of biasing the blending function can be seen as it enables the rate at which the final exit condition is achieved to be controlled.

When a helicopter experiences an engine failure after the TDP during a Towered Takeoff manoeuvre, piloting strategy dictates that the vehicle must adopt a new trajectory in the form of a recovery manoeuvre. An example of this type of recovery manoeuvre is shown in Figure 8. In this case, the engine failure occurs at  $t=15s$ , with pilot response time,  $t_r$ , specified to be five seconds. The manoeuvre exit height and flight path velocity were defined to be 25m below the rig height and 40kts respectively, while the exit rate of climb was equated to zero. It is evident Figure 8 that the recovery manoeuvres have been successfully evaluated for a range of  $\delta_x$ ,  $\delta_y$  and  $\delta_z$ . From Figure 9c, it can be seen that increasing values of  $\delta_z$  allows the exit height to be intercepted at an earlier stage thus effectively completing the manoeuvre.

Not only is it important for the mathematical description of the recovery manoeuvre to closely represent the actual flight path, but it must also encapsulate the





various pilot strategies used when an engine failure occurs during differing phases of the offshore operations considered in this study. For example, if a helicopter experiences an engine failure close to the oilrig platform during a landing manoeuvre, the proximity of the rig structure may influence pilot strategy so that heading and altitude become the key flight path parameters crucial to the safety of the helicopter. In the event of an engine failure towards the end of a towering takeoff manoeuvre, however, the influence of helicopter longitudinal velocity could be of prime concern in the piloting strategy. Therefore, the importance of single or multiple flight path parameters in the definition of the recovery trajectory can be accommodated by individually selecting the blending rate parameter,  $\delta$ , for each of the flight path constraints. This is demonstrated in Figure 10, where the longitudinal, lateral, altitude and heading flight path time histories, evaluated using separate values of the blending rate parameter, are shown. The figure clearly shows the importance of individually specifying the blending rate parameter for each of the four flight path constraints.

#### 4.0 Conclusions

A mathematical model of a torque limited, twin gas turbine power plant which has the ability to simulate an engine failure has been developed. The model's simple and efficient construction allows it to be readily employed in current flight mechanic simulation packages. With this model, it is now possible to represent the performance of actual helicopter powerplants under conditions of engine failure with some degree of confidence, and therefore the use of the engine model in future investigations will provide credence to any piloting strategies developed.

A novel hybrid simulation technique that utilises both inverse and forward methods has been developed. Termed HIFIS, the algorithm has an inverse - forward - inverse architecture allowing the simulation of engine failure flight while accommodating variations in pilot reaction time. The development of the HIFIS algorithm necessitated the generation of special flight paths that encapsulated piloting strategy in the event of the helicopter suffering an engine failure. The formulation of these recovery manoeuvres provide the degree of flexibility required in the evaluation of the recovery trajectories. Qualitative discussions between the University of Glasgow and the CAA have indicated that the recovery trajectories compare well with those found in current offshore operations.

When combining the engine model, the HIFIS algorithm and the recovery manoeuvre definition, it will be possible in future studies to confidently investigate





offshore operations under conditions of engine failure while obeying engine power limiting structures and accommodating variations in pilot response time and strategy.





## **Acknowledgements**

The authors would like to thank Mr. N. Talbot of the CAA for his advice with regard to the piloting aspects of helicopter offshore operations. With respect to engine modelling, the advice and enthusiasm given by Professor Maccallum of the Department of Mechanical Engineering was gratefully received.

This work was funded by the Civil Aviation Authority through the Air Registration Board Research Grant under contract number 7D/S/960.



## **References**

1. Taylor, C., Thomson, D.G., Bradley, R., 'Rotor Inflow Modelling Enhancements to Helicopter Generic Simulation Mathematical Model', Department of Aerospace Engineering, University of Glasgow, Internal Report No. 9215, September 1992.
2. Taylor, C., Thomson, D.G., Bradley, R., 'The Mathematical Modelling of Helicopter Offshore Manoeuvres', Department of Aerospace Engineering, University of Glasgow, Internal Report No. 9217, November 1992.
3. Thomson, D. G., Bradley, R., 'Development and Verification of an Algorithm for Helicopter Inverse Simulation', *Vertica*, Vol. 14, No. 2, pp. 185 -200, 1990.
4. Anon, 'British Civil Airworthiness Requirements Part 29', Civil Aviation Authority.
5. Trivier, D., Bosqui, D., '30 - Second/ 2 - Minute One Engine Inoperative Certification for the AS 332 Super Puma Mk 2', Eighteenth European Rotorcraft Forum, Paper 129, September 1992, France.
6. Thomson, D. G., 'Development of a Generic Helicopter Mathematical Model for Application to Inverse Simulation', Department of Aerospace Engineering, University of Glasgow, Internal Report No. 9216, March 1992.
7. Maccallum, N., 'Gas Turbine Transient Performance', Department of Mechanical Engineering, University of Glasgow, 1992.
8. Padfield, G. D., 'A Theoretical Model of Helicopter Flight Mechanics for Application to Piloted Simulation', Royal Aircraft Establishment, Technical Report 81048, April 1981.





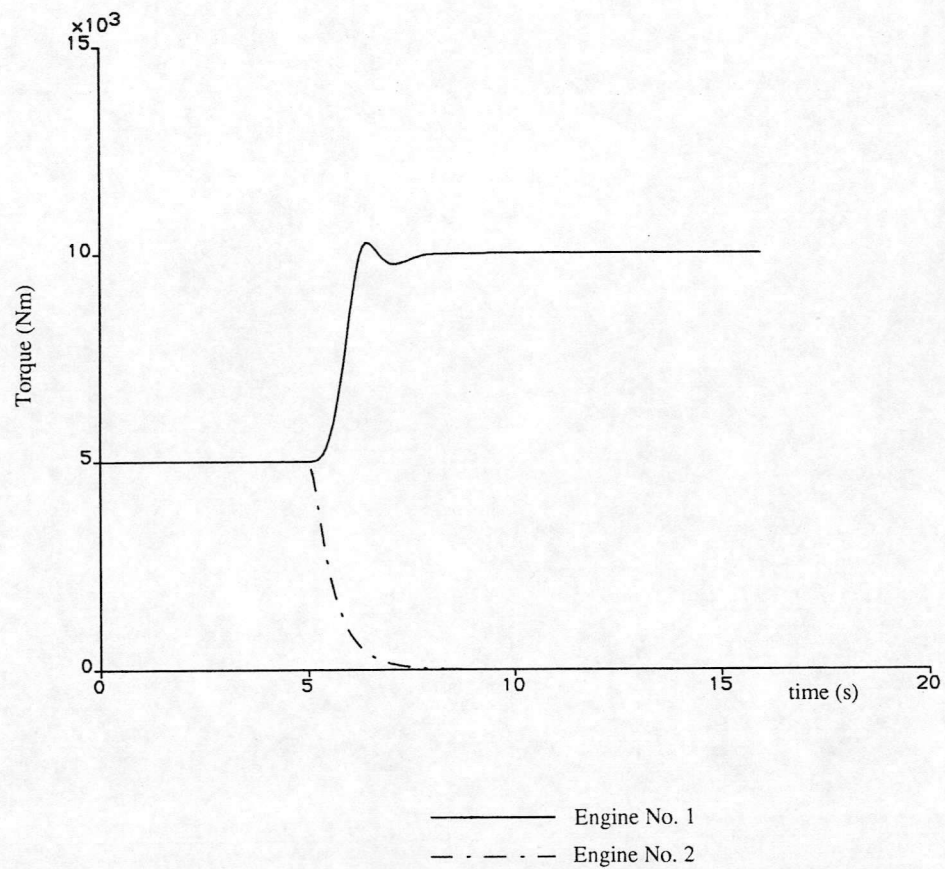


Figure 1 - Engine Torque Time History for Unlimited Torque Output  
No.1 Engine Failed at  $t=5.0$ s

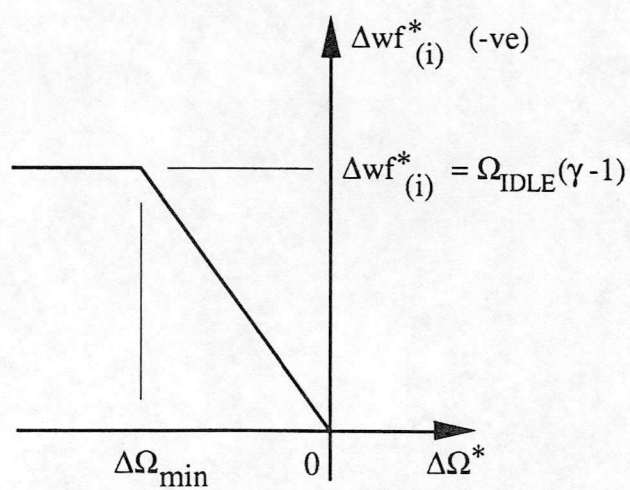


Figure 2 - Fuel Schedule as a Function of Rotor Speed





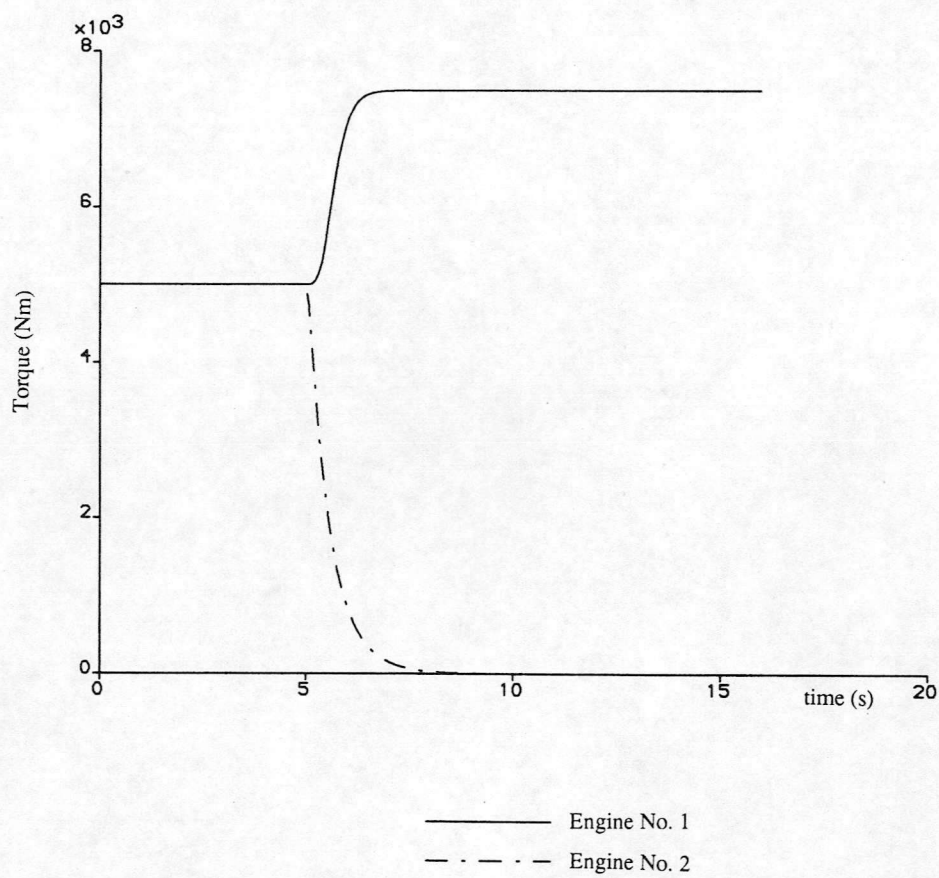


Figure 3 - Engine Torque Time History for Limited Torque Output  
No.1 Engine Failed at  $t=5.0s$



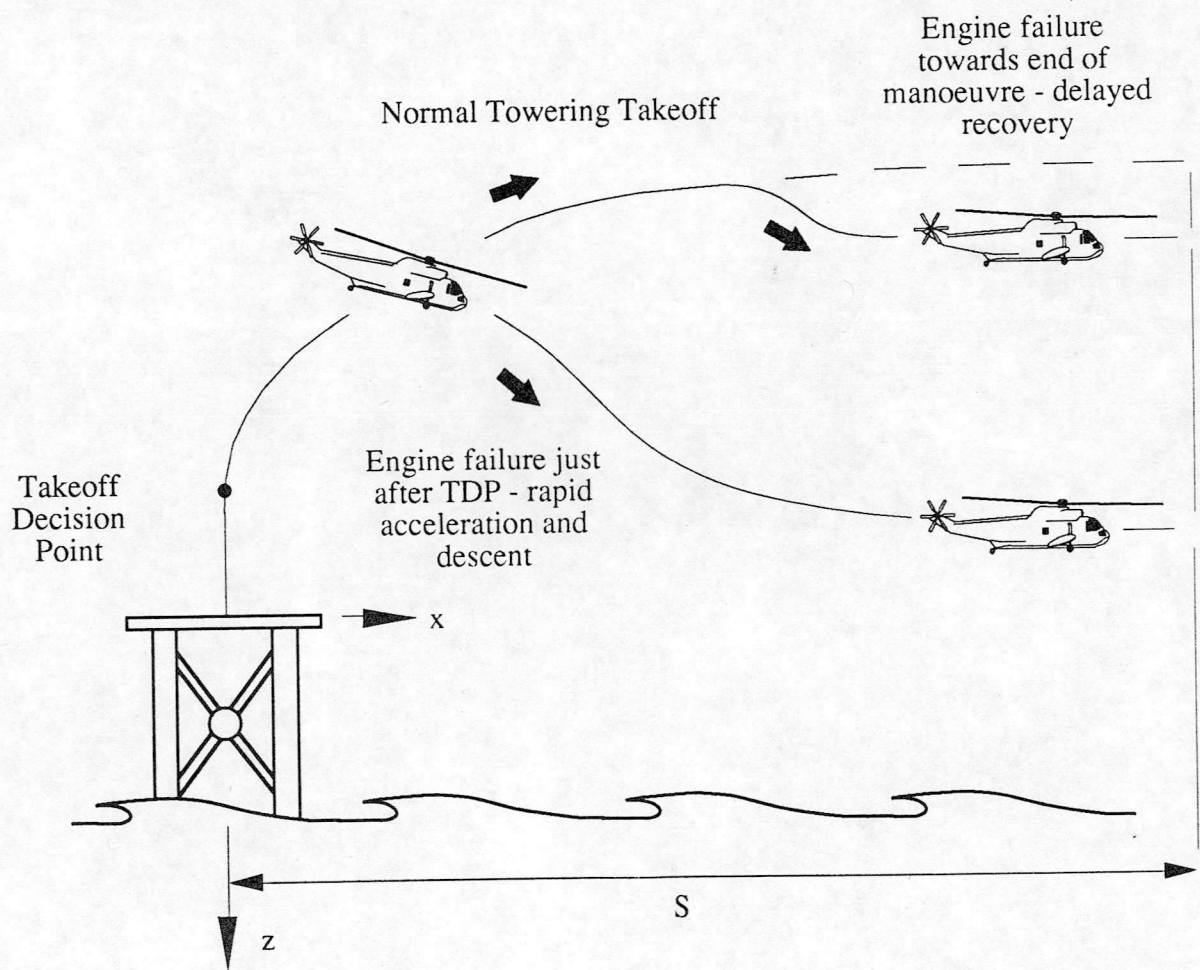


Figure 4 - Variation of Recovery Manoeuvre with Engine Fail Time





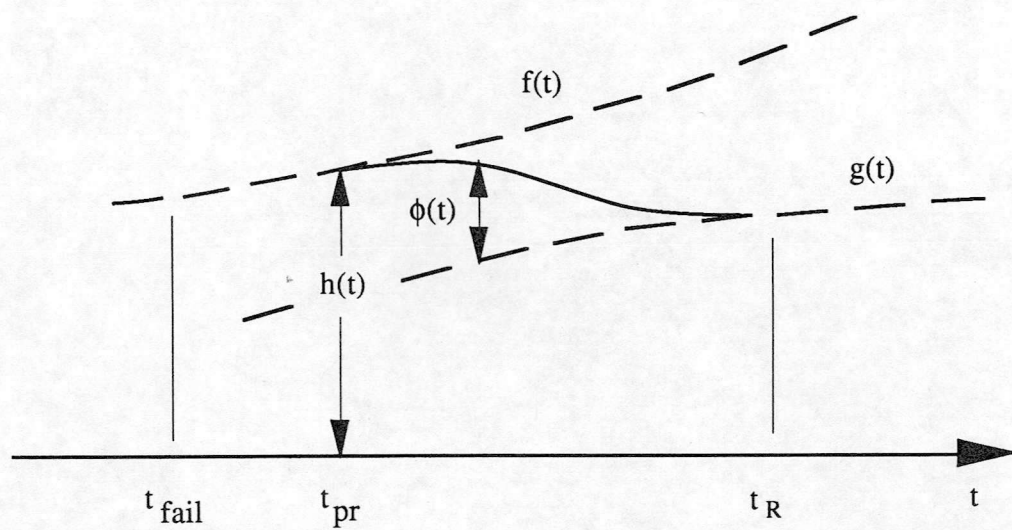


Figure 5 - Blending Flight Path





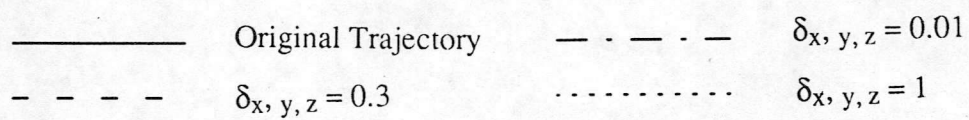
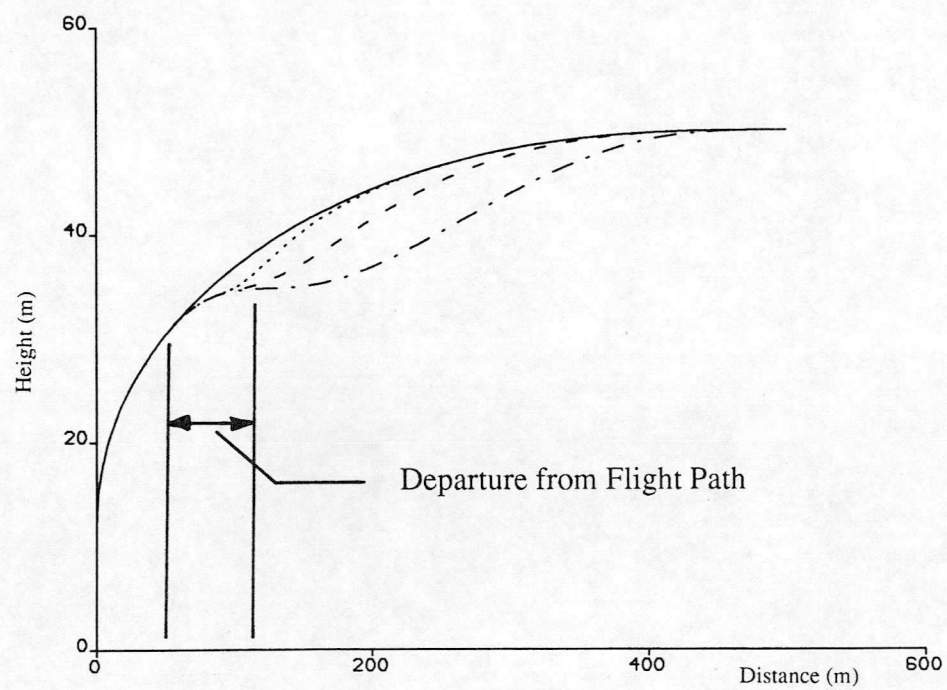


Figure 6 - Flight Path for Towering Takeoff



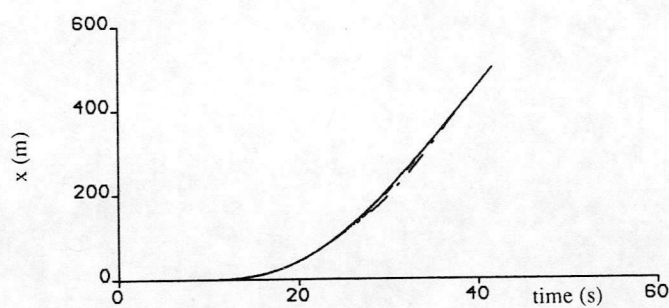


Figure 7a - Longitudinal Time History

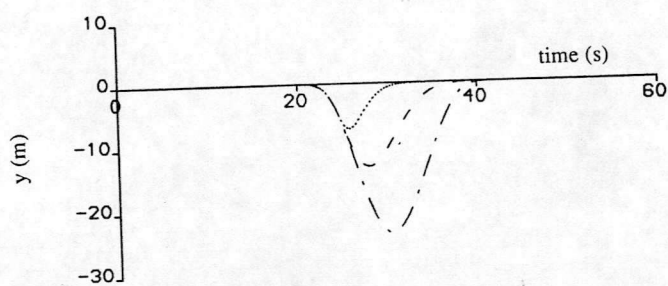


Figure 7b - Lateral Time History

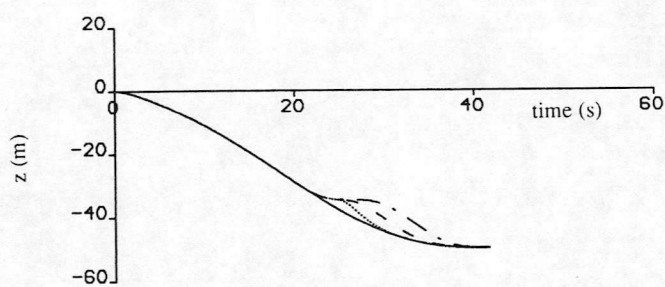


Figure 7c - Altitude Time History

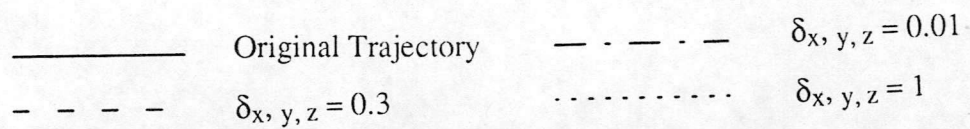


Figure 7 - Trajectory Components for Towering Takeoff





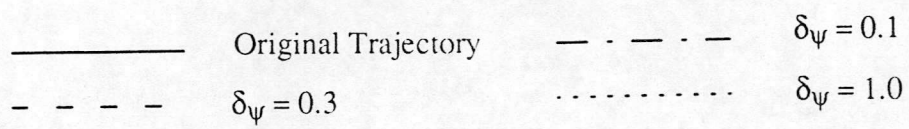
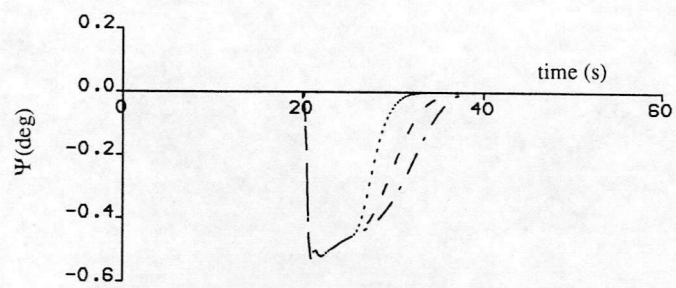


Figure 7d - Altitude Time History

Figure 7 - (Continued)





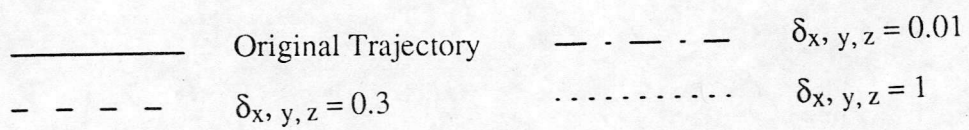
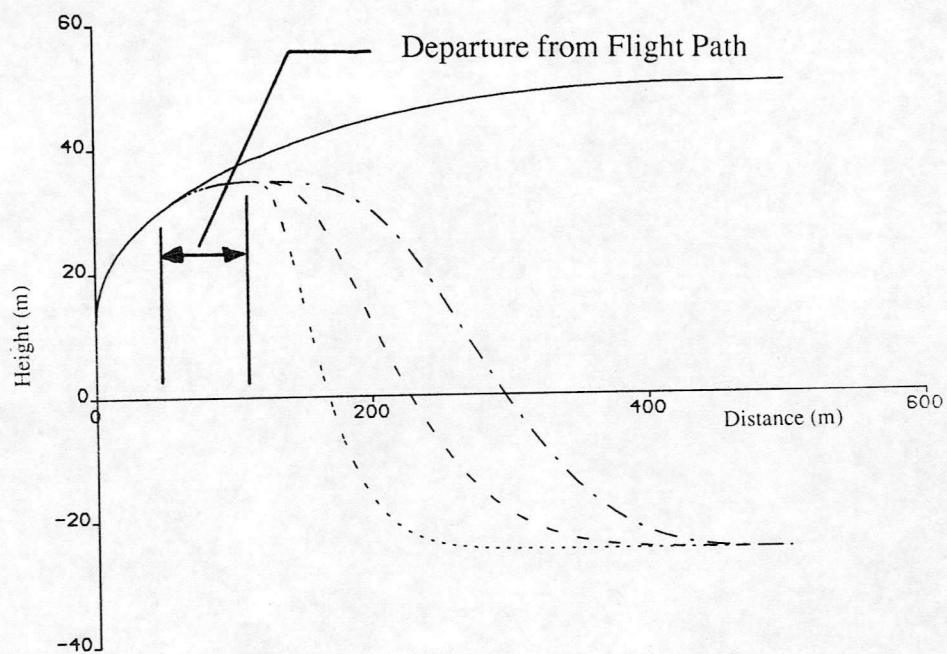


Figure 8 - Flight Path for Return to New Trajectory



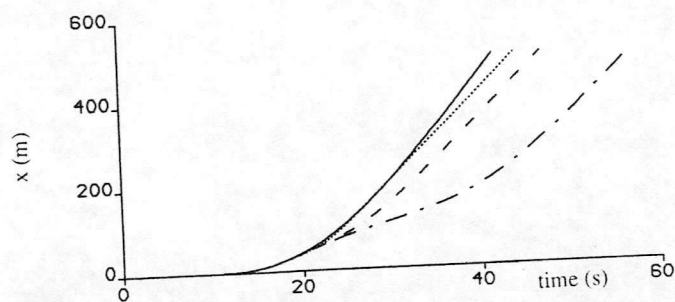


Figure 9a - Longitudinal Time History

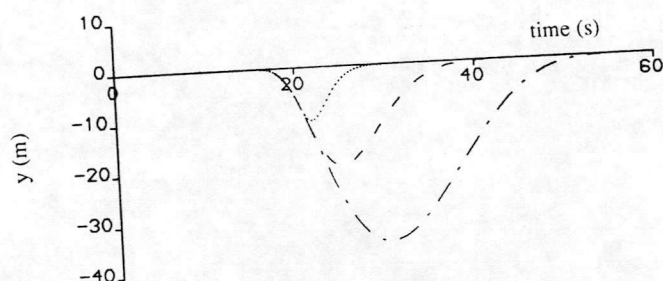


Figure 9b - Lateral Time History

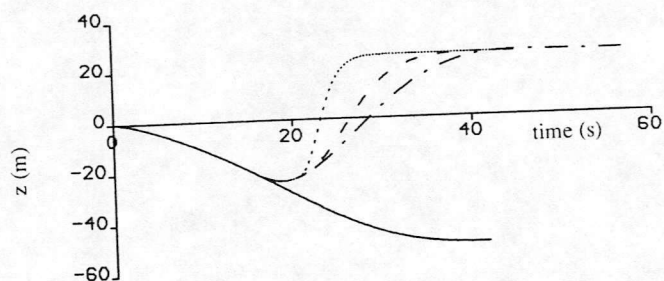


Figure 9c - Altitude Time History

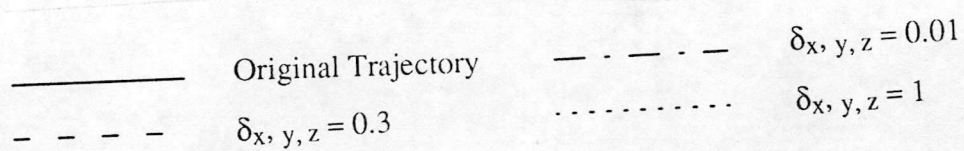


Figure 9 - Trajectory Components for New Trajectory





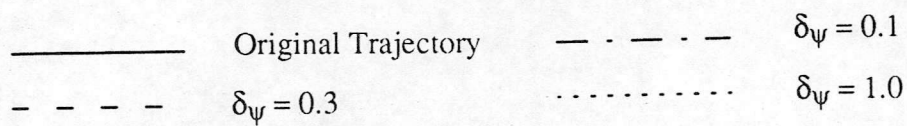
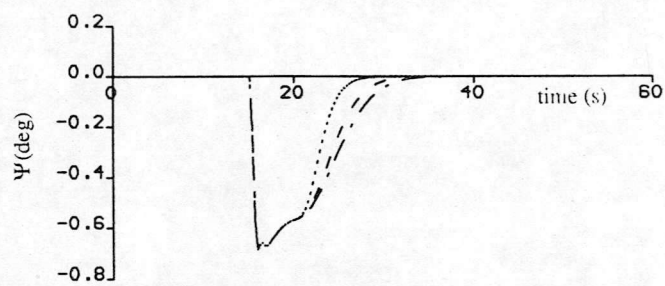


Figure 9d - Heading Time History

Figure 9 - (Continued)





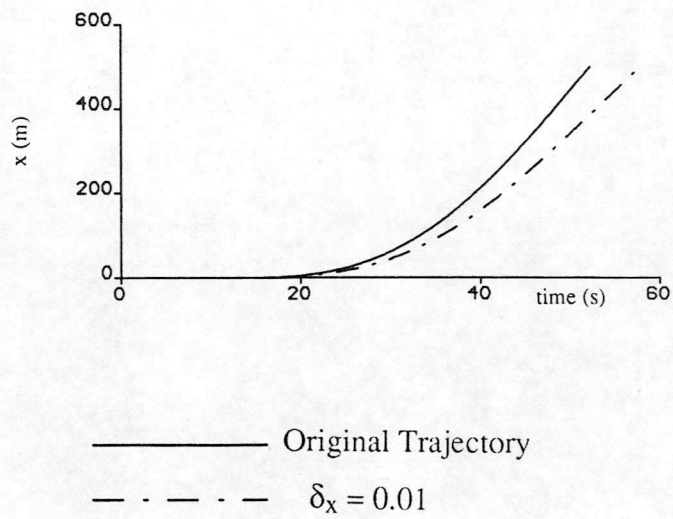


Figure 10a - Longitudinal Time History

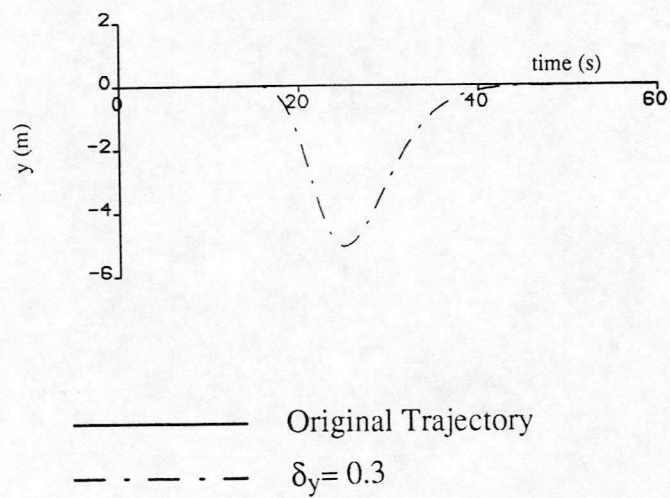


Figure 10b - Lateral Time History

Figure 10 - Tailoring of Individual Trajectory Components for New Trajectory



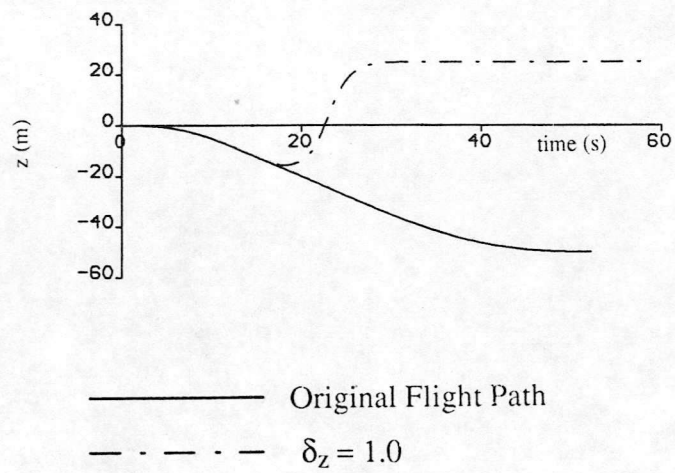


Figure 10c - Altitude Time History

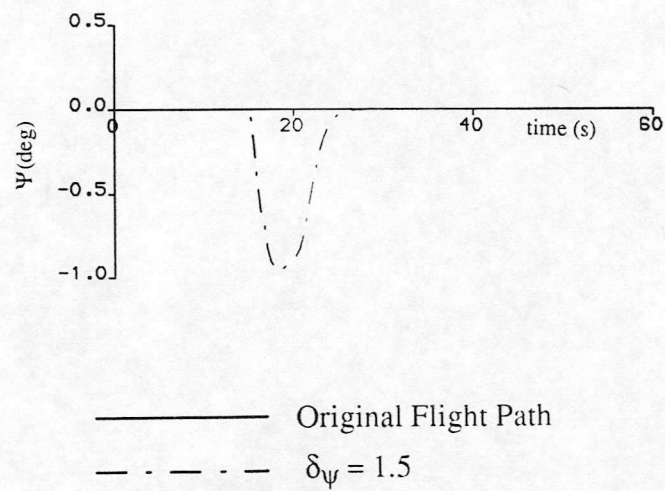


Figure 10d - Heading Time History

Figure 10 - (Continued)







